

Supplementary Materials

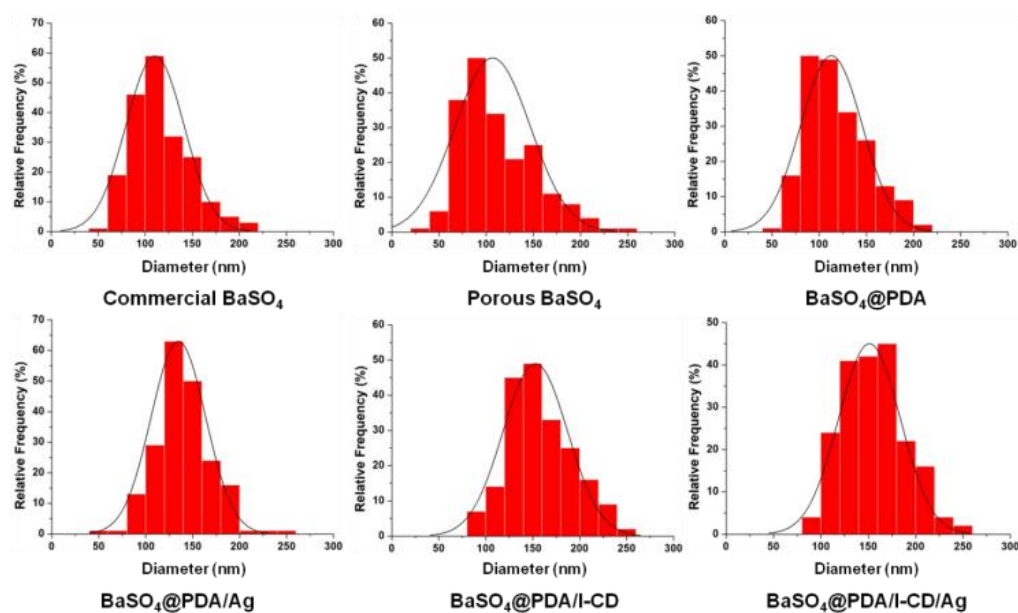


Figure S1. The diameter distribution of different microparticles.

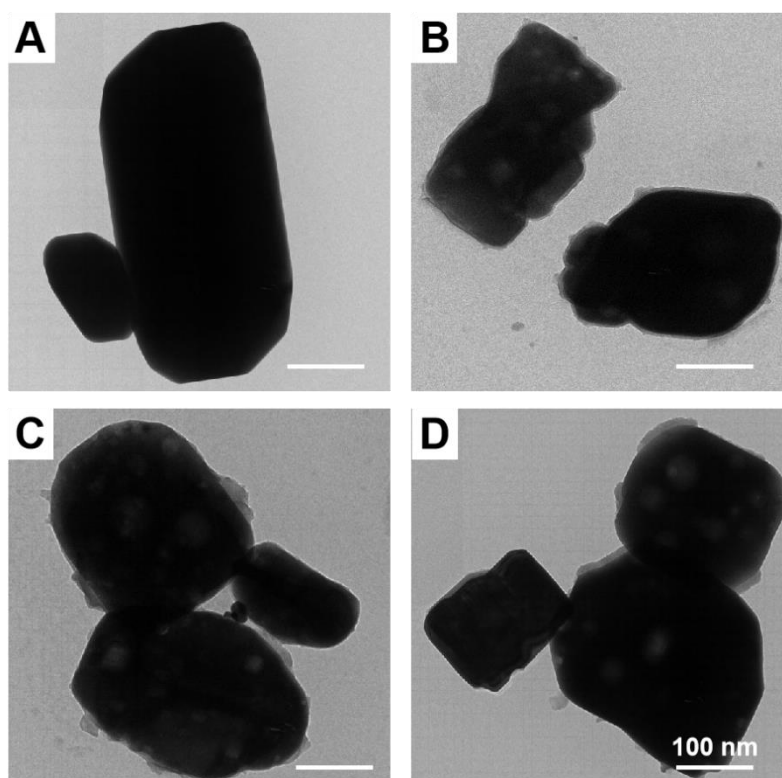


Figure S2. TEM images of (A) BaSO_4 ; (B) porous $\text{BaSO}_4@PDA$; (C) porous $\text{BaSO}_4@PDA/Ag$ and (D) porous $\text{BaSO}_4@PDA/I-CD/Ag$ microparticles.

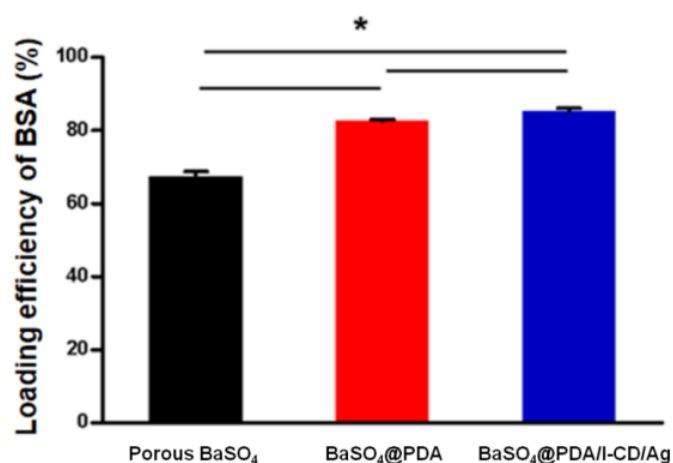


Figure S3. The loading efficiency of BSA in porous BaSO₄, BaSO₄@PDA and BaSO₄@PDA/I-CD/Ag particles. * $p < 0.05$.

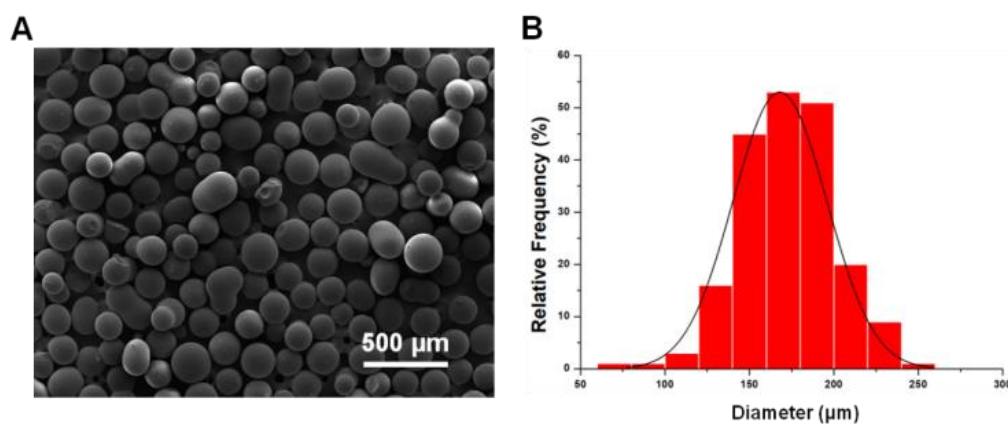


Figure S4. (A) SEM images of the PMMA for preparing bone cement. (B) The diameter distribution of PMMA particles.

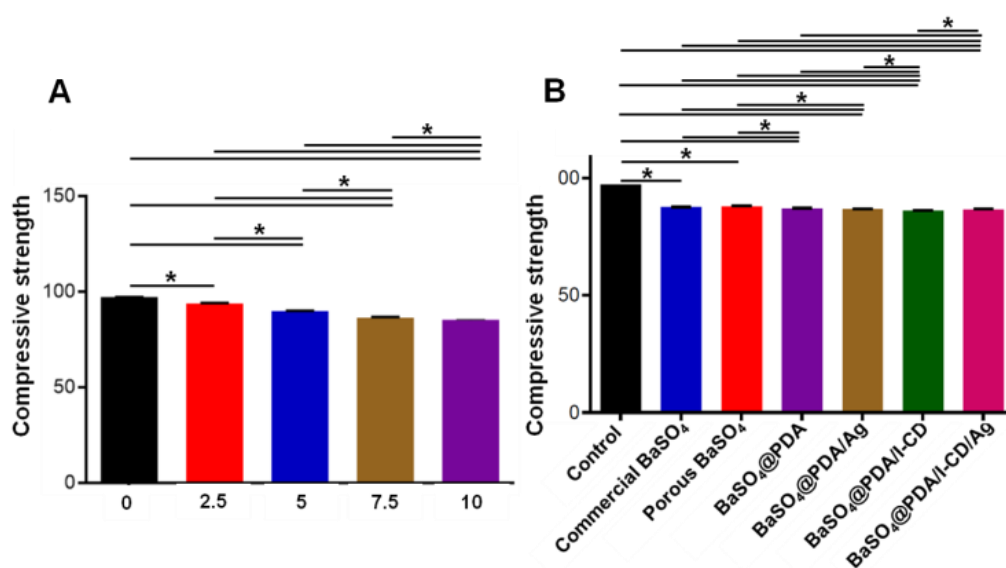


Figure S5. (A) Compressive strength of PMMA bone cements containing 0, 2.5 wt%, 5 wt%, 7.5 wt% and 10 wt% porous BaSO_4 @PDA/I-CD/Ag microparticles. (B) Compressive strength of PMMA bone cement (Control) and PMMA bone cements adding 7.5 wt% commercial BaSO_4 , porous BaSO_4 , BaSO_4 @PDA, BaSO_4 @PDA/Ag, BaSO_4 @PDA/I-CD and BaSO_4 @PDA/I-CD/Ag microparticles. $*p < 0.05$.

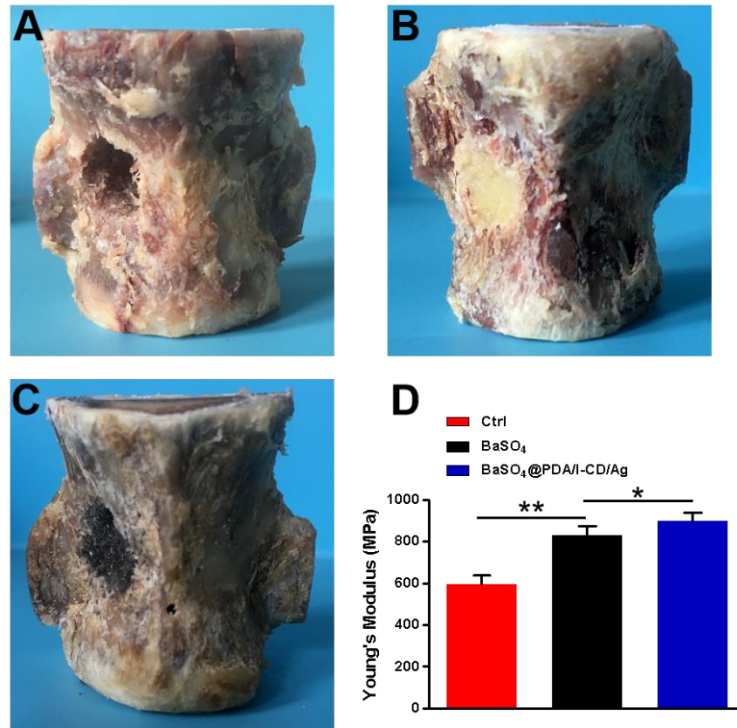


Figure S6. Images of sheep vertebral with defect as Ctrl group (A), and defects filled with PMMA bone cement containing commercial BaSO_4 particles (B) and BaSO_4 @PDA/I-CD/Ag particles (C). And Young's modulus of different groups (D). $*p < 0.05$.